

# Precipitation of Si revealed by dilatometry in Al-Si-Cu/Mg alloys

F. Lasagni\*, A. Falahati, H. Mohammadian-Semnani, H. P. Degischer

*Institute of Materials Science and Technology, Vienna University of Technology,  
Karlsplatz 13/E308, A-1040 Vienna, Austria*

Received 24 September 2007, received in revised form 5 October 2007, accepted 5 October 2007

## Abstract

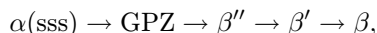
In this work, the precipitation sequence in different Al-alloys containing Si, Mg and/or Cu as major alloying elements is investigated by differential scanning calorimetry (DSC) and dilatometric tests. The superposed exothermic and endothermic effects due to the precipitation and dissolution of Si are separated by the temperature dependence of the instantaneous coefficient of thermal expansion (CTE) from the precipitation sequence of  $\theta''/\theta$  and  $\beta$  precipitates of the age hardening elements. Vacancy annihilation during heating of quenched samples can only be observed by dilatometry of the Si-free alloys.

**Key words:** Al-alloys, precipitation kinetics, thermal expansion, differential scanning calorimetry (DSC), dilatometry

## 1. Introduction

Most of the casting Al-alloys contain between 5–22 % Si which improves the castability. Al-Si alloys are well known for applications in combustion engines because of their good thermal conductivity and low thermal expansion [1]. Dimensional stability is of importance in engine components, which are exposed to thermal cycling. Residual length changes in motor components would produce internal stresses affecting the service life of components.

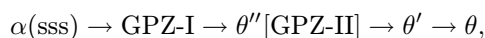
Wrought Al-alloys of the Al-Si-Mg system are now being used increasingly for car body components and are subject of several studies [2–5]. The strengthening of Al-Mg-Si alloys is based on precipitation hardening by [6]:



where  $\alpha(\text{sss})$  is the supersaturated solid solution; GPZ-zones are generally considered spherical clusters of Mg and Si atoms with undefined structure;  $\beta''$  are fine needle-shape precipitates;  $\beta'$  are rod-shaped precipitates having a hexagonal crystal structure, and the  $\beta$  phase is usually segregated as  $\text{Mg}_2\text{Si}$  platelets.

The addition of Cu to Al-Si system improves strength and machinability of alloys at the expense

of reduced castability, ductility and corrosion resistance. Casting alloys with compositions within ranges of 3–10.5 % silicon and 1.5–4.5 % copper have been developed where a compromise between these properties is reached. To date, the precipitation sequence of Al-Cu and Al-Cu-Mg alloys is well stated as [6]:



where GPZ-I stands for monolayer Cu-rich zones;  $\theta''$  are bilayer and multilayer structures;  $\theta'$  is a metastable phase (planar precipitates); and  $\theta$  are precipitates of the  $\text{Al}_2\text{Cu}$ -composition (intermetallic phase) [7, 8]. In Al-Cu-Mg alloys phases  $\theta''$ ,  $\theta'$  and  $\theta$  are replaced by  $S''$ , semicoherent  $S'$  and stable  $S$  (orthorhombic  $\text{CuMgAl}_2$ ) [9].

Further investigations have been carried out in order to understand the influence of Si and Cu on the precipitation sequence in Al-Mg-Si and Al-Si-Cu alloys [4, 10, 11]. Usually, the precipitation of Si is reported to be superposed to the formation of  $\beta$  or  $\theta$  precipitates. Therefore, its effect on the precipitation sequence of alloys has been hardly observed [3, 4, 11]. The present work will enhance the understanding of the precipitation kinetics of Si in Al-Si-Mg and Al-Si-Cu alloys as well as the influence of previous thermal treatment. Wrought and casting alloys were subjected

\*Corresponding author: tel.: +34 91444 1518; fax: +34 91445 1764; e-mail address: [flasagni@hotmail.com](mailto:flasagni@hotmail.com)

Table 1. Composition of main components of the studied alloys (wt.%)

Alloy	Si	Mg	Cu	Fe
AlSi1Mg0.4	1.00	0.43	0.03	0.26
AlSi8Mg5 [12]	8.40	4.9	< 0.01	0.5
AlMg5.5Si2.5 [12]	2.46	5.50	< 0.01	< 0.15
AlSi8Cu3.5	8.05	< 0.001	3.39	0.07
AlCu4Mg1	0.2	1.37	3.70	0.09
AlSi1.1 [14]	1.11	0.003	< 0.01	0.09
AlSi1.7 [14]	1.74	0.001	< 0.01	0.07

to dilatometric and calorimetric (DSC) experiments during linear heating and compared with each alloy. The thermal expansion of these alloys is quantified and related to the precipitation of supersaturated Si and distinguished from other precipitates.

## 2. Experimental methods

The AlSi8Cu3.5 alloy was produced using a squeeze casting process by LKR, Austria. The strip cast AlMg5.5Si2.5 was provided by ALCAN, CRV, France and the AlSi8Mg5 samples were produced by laboratory gravity casting at GPM2/INP-Grenoble, France [12]. The strip cast AlSi1Mg0.4 and hot rolled AlCu4Mg1 (2024) alloys were provided by AMAG-Rolling, Austria. The compositions of the studied materials are depicted in Table 1. Further information on the AlSi alloys as well as experimental details are given in [13].

Samples of  $15 \times 4 \times 2 \text{ mm}^3$  size with parallel smoothed faces were prepared in order to perform dilatometric measurements in a TMA equipment (Thermo-Mechanical Analyser 2940 CE). DSC measurements were performed in a DSC2920 equipment using samples of 6 mm diameter and 1 mm thickness ( $\sim 80 \text{ mg}$  mass) vs. 99.99 % pure-Al. Both DSC and dilatometric measurements were performed using a heating rate of  $5 \text{ K min}^{-1}$  in nitrogen atmosphere. The alloys were tested in the T4 condition after solution treatment (ST:  $540^\circ\text{C}/1 \text{ h}$  for Al-Si-Mg; and  $520^\circ\text{C}/1 \text{ h}$  for Al-Cu-Mg/Si alloys followed by water quenching) and by a second cycle after moderate cooling rates from  $540^\circ\text{C}$  or  $520^\circ\text{C}/15 \text{ min}$  to room temperature at cooling rates of 20, 5 or  $3 \text{ K min}^{-1}$  (denominated T4a, T4b and T4c, respectively). The instantaneous CTE at temperature  $T$  was calculated from the  $\Delta l(T)$ -curves by means of the numerical derivative smoothed within intervals of  $T \pm 12.5 \text{ K}$  as:

$$\text{CTE}(T) = \frac{1}{L} \frac{dL}{dT}, \quad (1)$$

where  $L$  is the length of the specimen at the respective temperature  $T$ .

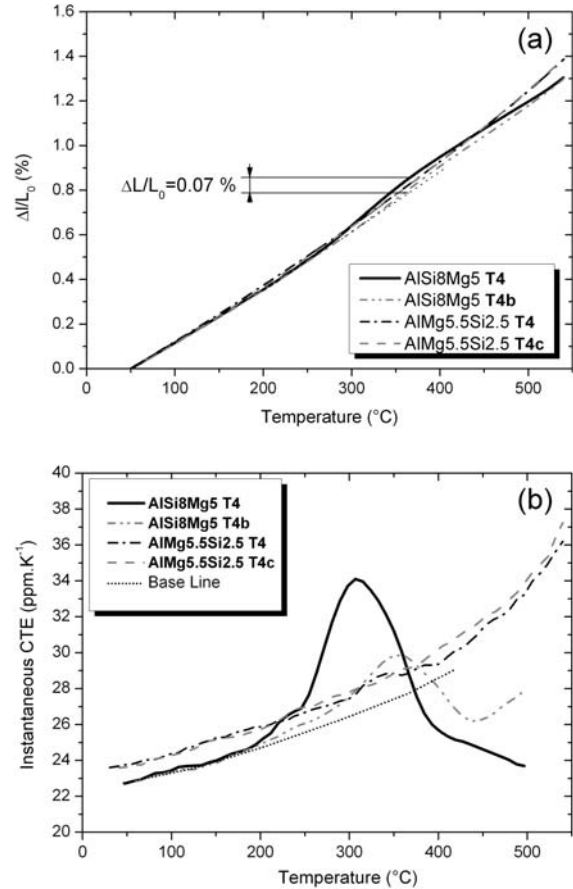


Fig. 1. Thermal expansion (a) and CTE vs. temperature (b) of AlSi8Mg5 and AlMg5.5Si2.5 alloys after water quenching (T4) and slowly cooled conditions from solution treatment (T4b:  $5 \text{ K min}^{-1}$ , T4c:  $3 \text{ K min}^{-1}$ ).

## 3. Results and discussion

The linear expansion of the AlSi8Mg5 and AlMg5.5Si2.5 alloys in the T4 (water quenched) and T4b (slowly cooled at  $5 \text{ K min}^{-1}$  from ST) conditions is depicted in Fig. 1a. The AlSi8Mg5 sample presents additional expansion of about 0.07 % between 200 and  $360^\circ\text{C}$  in the T4 condition (comparable to that of Al-Si alloys containing  $> 1.7 \%$  [14]), while the T4b condition (slowly cooled at  $5 \text{ K min}^{-1}$ ) expands almost linearly with increasing temperature. This effect is clearly observed from the  $\text{CTE}(T)$  in Fig. 1b, where a higher  $\text{CTE}(T)$  peak can be observed in the T4 condition due to increasing volume fraction of precipitated Si. It is important to note that the CTE peak observed at  $355^\circ\text{C}$  in T4b appears at lower temperature if compared with samples of the Al-Si-system ( $\sim 380^\circ\text{C}$ ) [14]. This effect is related to heterogeneous nucleation of Si in absence of vacancy supersaturation.  $\text{Mg}_2\text{Si}$  precipitates provide stable nuclei for the precipitation of Si at lower temperatures than in pure Al-Si system. The  $\text{CTE}(T)$  of T4 and T4b conditions decreases below

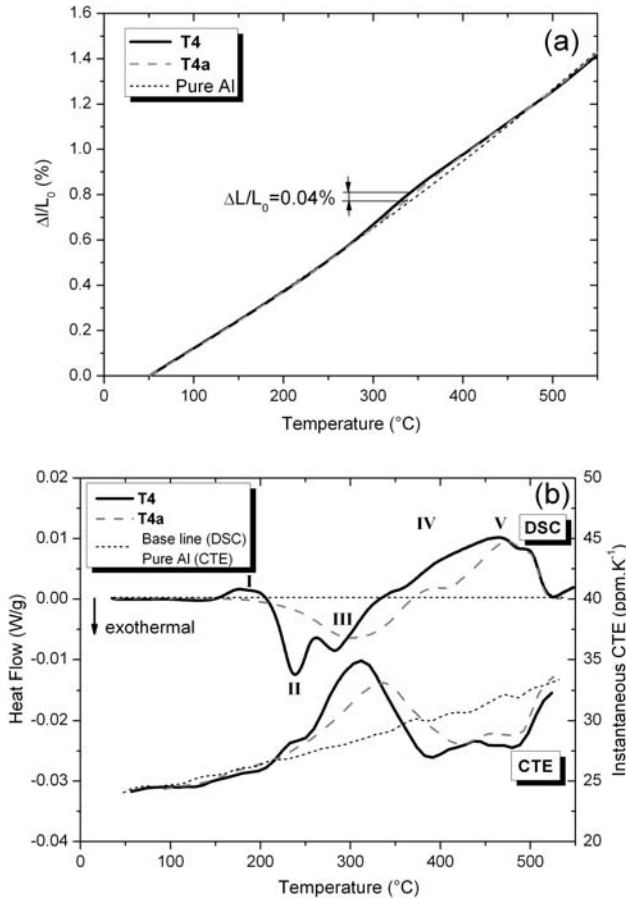


Fig. 2. Thermal expansion (a) and CTE( $T$ ) and DSC runs (b) of an AlSi1Mg0.4 alloy after different thermal conditions (for explanation see text).

the base line (parallel to that of AlMg5.5Si2.5) due to the dissolution of the Si precipitates above 370 and 395 °C, respectively, as discussed in [14]. On the other hand, the thermal expansion of AlMg5.5Si2.5 in both T4 and T4c (slowly cooled at 3 K min<sup>-1</sup>) conditions increases with temperature almost linearly. Since the Si content is below the stoichiometric composition, it is consumed by the formation of Mg<sub>2</sub>Si precipitates which produce neither an additional expansion in the alloy around 300 °C, nor dissolution of Si above 350 °C.

The linear expansion of AlSi1Mg0.4 alloy in water quenched (T4) and slowly cooled sample at 20 K min<sup>-1</sup> (T4a) conditions is illustrated in Fig. 2a. Both water quenched and slowly cooled samples present an additional expansion around 300 °C of 0.04 % and 0.025 %, respectively. Like in AlSi8Mg5, the reduction of the cooling rate produces a displacement in the CTE( $T$ ) peak from 310 °C for T4 to 335 °C for T4a condition (Fig. 2b). Both are related to the precipitation of Si into diamond structure. The DSC runs of the studied alloy in T4 and T4a conditions are in agreement with those reported by [4, 10, 15].

The DSC curve in T4 shows two exothermic peaks II and III, and two endothermic effects I and V. The last one is superposed with an exothermic formation marked by IV. The trough I, exhibiting a maximum at 183 °C, is consistent with the dissolution of some of the GP-zones and clusters that are typically present in the T4 condition. Subsequently, an exothermic effect is observed at 240 °C (peak II), which is related with the formation of needle-like  $\beta''$  precipitates. This peak is followed by the exothermic formation of more stable rod-shape  $\beta'$  simultaneously with Si precipitates, which is also observed by dilatometry at the same temperature range (peak III, 282 °C). After that, the endothermic dissolution of Si precipitates is superposed with the formation of stable Mg<sub>2</sub>Si- $\beta$  precipitates at 348 °C, marked IV. At higher temperatures, only the dissolution of  $\beta$  and Si precipitates is observed (peak V) reaching complete solid solution at about 500 °C.

For the slowly cooled sample (T4a) it is not surprising that both peaks I and II disappear in the thermogram, since Mg<sub>2</sub>Si-precipitates are already formed during cooling. Therefore the observed exothermic peak at 302 °C (peak III) is related to further formation of Mg<sub>2</sub>Si, and the growth of Si-precipitates, both increasing their volume fraction (as observed for Si by dilatometry). The formation of stable  $\beta$  precipitates is superposed with the endothermic dissolution of Si (around IV) like in T4, but at a slightly higher temperature (408 °C) indicating higher diameters. Above 450 °C, the dissolution of Mg<sub>2</sub>Si and Si precipitates is observed in the same way as for the T4 samples.

DSC runs of an AlCu4Mg1 sample in the T4 and T4a conditions are depicted in Fig. 3a and they are in agreement with those reported by [9]. Three endothermic and two exothermic effects are observed in the T4 condition. Peaks I and II are related to the dissolution of single- and multilayer GP-zones, respectively [16]. The two overlapped exothermic peaks IV and V recorded at 260 and 276 °C are related to the formation of  $\theta''$  and  $\theta'$  phases, respectively. According to Badini et al. [9] the formation of  $\theta'$  and  $S'$  phases may be overlapped in this alloy and observed in peak V during DSC runs. After that, a large endothermic effect is observed from about 305 °C, where dissolution phenomena ( $\theta' + \theta$  phases) and precipitation of  $\theta$  occur (peak VI). The slowly cooled sample (T4a) presents an endothermic effect at 224 °C (III) which is referred to the dissolution of  $\theta''$  precipitates. After that, the formation of  $\theta'$  and  $S'$  phases appears to occur simultaneously between 254–333 °C (V) and the dissolution of the formed precipitates overlapped with formation of  $\theta$  is observed afterwards (VI). The determined CTE increases linearly with temperature and is comparable to that of pure-Al in the slowly cooled conditions (T4a, b).

At the temperature of the thermal effects IV and

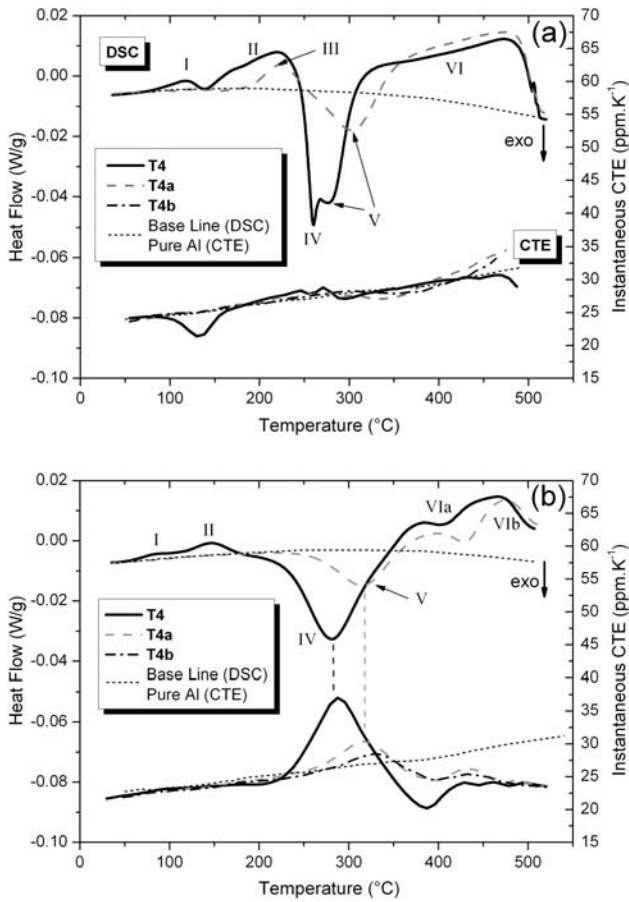


Fig. 3. DSC runs and CTE extracted from dilatometric tests both at  $5 \text{ K min}^{-1}$  heating rate in AlCu4Mg1 (a) and AlSi8Cu3.5 (b) alloys after different cooling rates from solution treatment (for explanation see text).

V, there are very small maxima in the CTE which are not yet explained. Only a drop of the CTE in the supersaturated T4 condition is recorded between 90–170°C (range of GPZ I, II formation), which is correlated with the loss of supersaturated vacancies. The observed linear length change between RT and 170°C for the quenched AlCu4Mg1 samples amounts to a con-

traction of  $1.3 \times 10^{-4}$ . The vacancy supersaturation by quenching from 520°C corresponds to a volume of  $3 \times 10^{-4}$  [17] yielding a linear contraction of  $10^{-4}$  as soon as they are annihilated. The precipitation of Cu platelets produces much less contraction perpendicular to their habit planes ( $\sim 10^{-5}$ ). The CTE-Minimum L is mainly caused by the annihilation of supersaturated vacancies which are repelled by vacancy type GPZ.

The calorimetric curves performed in an AlSi8Cu3.5 alloy are somehow different to those of the AlCu4Mg1 alloy (Fig. 3b). As observed before, the endothermic effects I, II seem to be related to the dissolution of the different GP-zones of the T4 condition. Contrary to AlCu4Mg1, a single exothermic effect at 280°C is observed in T4 (peak IV), which is shifted to higher temperatures (peak V: 315°C) in the slowly cooled sample (T4a). These thermal effects (IV and V) are correlated with the CTE peaks measured during dilatometry tests, and therefore, may be related to the precipitation of Si simultaneously with the  $\theta'$  or  $S'$  phases which may also act as heterogeneous nuclei during Si precipitation. The CTE minimum observed for AlCu4Mg1 around 130°C cannot be observed in the Si containing alloy. Two endothermic effects (VIa,b) are observed from about 350°C in both T4 and T4a thermal conditions and correlated with the drop in the CTE curve below ROM (Al+6.8%Si). These may be related to the dissolution of precipitates formed at peak IV and V, respectively, but predominantly for Si precipitates.

Table 2 depicts the experimental and calculated thermal expansion of the studied alloys in the water quenched condition. The theoretical linear expansion due to the precipitation of Si is estimated by:

$$\Delta l_{\text{mod}} = \frac{(V_{\text{atSi}} - V_{\text{atAl}})}{3 \cdot V_{\text{atAl}}} f \cdot 100 \%, \quad (2)$$

where  $V_{\text{atSi}}$  and  $V_{\text{atAl}}$  are the atomic volumes of Al (fcc) and Si (diamond structure), respectively, and  $f$  is the concentration of Si in supersaturation. Note that a

Table 2. Experimental and calculated additional expansion by Si precipitation in the studied alloys in T4 condition

Alloy	Si for $\text{Mg}_2\text{Si}$ (at.%)	Si excess (at.%)	Max. diss. (at.%) (Si-0.5Mg)	$\Delta l_{\text{calc.}}$ (%)	$\Delta l_{\text{exp.}}$ (%)	$\Delta V$ (%)
AlSi1Mg0.4	0.24	0.72	0.48*	0.035	0.04	0.12
AlSi8Mg5	2.35	5.34	0.90*	0.065	0.07	0.21
AlMg5.5Si2.5	> 2.28	0	0*	0	0	0
AlSi8Cu3.4	–	7.92	0.94 *at 520°C	0.67	0.8	0.24
AlCu4Mg1	–	–	–	0	0	0
AlSi1.1 [14]	–	1.06	1.06	0.075	0.07	0.21
AlSi1.7 [14]	–	1.63	1.13	0.081	0.08	0.24

\*estimated by Thermocalc<sup>®</sup>

maximum of about 0.94 and 1.13 at.% Si can be only dissolved in Al at 520 and 540 °C, respectively [14].

The results are in perfect agreement with the experimental data obtained for the T4 condition. The smaller expansion in the AlSi1Mg0.4 alloy is due to the lower Si content, while the maximum Si supersaturation in AlSi8Mg5, AlSi1.7 and AlSi12 is the same. Therefore, the measured additional expansion of the mentioned alloys yields the same values. No additional expansion is observed in both AlCu4Mg1 and AlMg5.5Si2.5 alloys. Neither the precipitation of Cu nor that of Mg<sub>2</sub>Si produce effects on thermal expansion. AlCu4Mg1 does not contain Si and AlMg5.5Si2.5 does not contain free Si as the Si content is below the stoichiometric composition for Mg<sub>2</sub>Si of the alloy and the solubility of Si (> 350 °C) is related with that of Mg forming again Mg<sub>2</sub>Si after quenching.

#### 4. Conclusions

Fast quenching of Al-Si-based alloys causes Si and vacancy supersaturation. Due to Si precipitation during slow heating an additional expansion around 300 °C (compared with the thermal expansion of pure Al or for Al-Si alloys with the eutectic Si according to ROM) takes place for water quenched Al-Si, Al-Si-Cu alloys and Al-Si-Mg with Si in excess of the stoichiometric Mg<sub>2</sub>Si concentration. The additional expansion is directly related with the Si supersaturated above the Mg<sub>2</sub>Si stoichiometry by quenching from solution treatment temperatures (> 350 °C). By decreasing the cooling rate from solution treatment the measured peaks observed in both CTE(*T*) and DSC curves are displaced to higher temperatures (between 300 and 350 °C) due to different modifications [14]. The difference in nucleation with and without vacancy supersaturation is presented in [18]. The magnitudes of these effects decrease indicating a reduction of the Si supersaturation owing to slow cooling. Mg<sub>2</sub>Si and Al-Cu precipitation does not produce any effect on the thermal expansion of Al-alloys, except a slight CTE decrease in AlCu4Mg1. The annihilation of quenched in vacancies cannot be observed in Si containing alloys. Si-vacancy clusters act as nuclei for platelet Si precipitates on {111} planes [18]. Whereas the supersaturated vacancies in Al-Cu alloys annihilate simultaneously to the dissolution of Cu GPZ, which is revealed by the comparison of the DSC thermogram with temperature dependence of the CTE.

The thermal expansion and the CTE(*T*) of all Si-containing alloys decrease at least above 400 °C with respect to that of pure Al due to the dissolution of Si. Si precipitation is only possible if supersaturation can be achieved up to the maximum solubility at solution treatment temperature (see Table 2). The effect of Si precipitation and dissolution can be identified in DSC

scans of Al-Si-Cu/Mg alloys by comparison with the calculated CTE(*T*) from dilatometric measurements. In this way, the precipitation kinetics of Si can be distinguished from the formation of β or β', and θ or θ' precipitates, respectively.

#### Acknowledgements

The authors acknowledge the provision of samples by ALCAN CR-Voreppe/France, AMAG-Rolling/Austria and Leichtmetall-Kompetenzzentrum Ranshofen/Austria, as well as Jorge Acuña for sample preparation for dilatometric tests in AlSiCu alloys.

#### References

- [1] DAVIS, J. R.: ASM Specialty Handbook: Aluminium and Aluminium Alloys. Materials Park, OH, USA, ASM International 1994.
- [2] EDWARDS, G. A.—STILLER, K.—DUNLOP, G. L.—COUPER, M. J.: Acta Mater., 46, 1998, p. 3893.
- [3] MATSUDA, K.—SAKAGUCHI, Y.—MIYATA, Y.—UTENI, Y.—SATO, T.—KAMIO, A.—IKENO, S.: J. Mater. Sci., 35, 2000, p. 179.
- [4] GUPTA, A. K.—LLOYD, D. J.—COURT, S. A.: Mater. Sci. Eng., A316, 2001, p. 11.
- [5] KARNTHALER, H. P.—WAITZ, T.—RETENBERGER, C.—MIGLER, B.: Mater. Sci. Eng., A387–389, 2004, p. 777.
- [6] MACKENZIE, D. S.—TOTTEN, G. E.: Analytical Characterization of Aluminium, Steel and Superalloys. Florida, CRC Press, Taylor & Francis Group 2006.
- [7] HATCH, J. E.: Aluminium Properties and Physical Metallurgy. Metals Park Ohio, American Society of Metals 1988.
- [8] VAITHYANATHAN, V.—WOLVERTON, C.—CHEN, L. Q.: Acta Mater., 52, 2004, p. 2973.
- [9] BADANI, C.—MARTINO, F.—VERNÉ, E.: Mater. Sci. Eng., A191, 1995, p. 185.
- [10] MIAO, W. F.—LAUGHLIN, D. E.: Scripta Mater., 40, 1999, p. 873.
- [11] WANG, G.—BIAN, X.—WANG, W.—ZHANG, J.: Mater. Lett., 57, 2003, p. 4083.
- [12] DEGISCHER, H. P.—KNOBLICH, H.—KNOBLICH, J.—MAIRE, E.—SALVO, L.—SUERY, M.: In: Proceedings: 12. Internationale Metallographie Tagung – Prak. Met. Sonderband 38. Eds.: Petzow, G., Kneissl, A. Leoben, Department Metallkunde u. Werkstoffprüfung & Germany Society of Materials (DGM) 2006, p. 67.
- [13] LASAGNI, F.: The role of Si on the microstructure of Al casting alloys and short fibre composites. [PhD thesis]. Vienna, Vienna University of Technology 2006.
- [14] LASAGNI, F.—DUMONT, M.—SALOME, C.—ACUÑA, J. A.—DEGISCHER, H. P.: Int. J. Mater. Res., 2008 (submitted).
- [15] HÄLLDAHL, L.: Thermochemica Acta, 214, 1993, p. 33.
- [16] AUVRAY, X.—GEORGOPOULOS, P.—COHEN, J. B.: Acta Metall., 29, 1981, p. 1061.

- [17] SHEWMON, P. G.: Diffusion in Solids. New York, McGraw-Hill 1963.
- [18] LASAGNI, F.—MINGLER, B.—DUMONT, M.—DE-GISCHER, H. P.: Mater. Sci. Eng. A, 2007 (in press).